Unsteady Transonic Flow Analysis for Low Aspect Ratio, Pointed Wings

K. R. Kimble,* D. D. Liu,† S. Y. Ruo,‡ and J. M. Wu§
The University of Tennessee Space Institute, Tullahoma, Tenn.

Oswatitsch and Keune's parabolic method for steady transonic flow is applied and extended to thin slender wings oscillating in the sonic flowfield. The parabolic constant for the wing was determined from the equivalent body of revolution. Laplace transform methods were used to derive the asymptotic equations for pressure coefficient, and the Adams-Sears iterative procedure was employed to solve the equations. A computer program was developed to find the pressure distributions, generalized force coefficients, and stability derivatives for delta, convex, and concave wing planforms. Input for the program includes planform shape, acceleration constant, pitch axis location, and frequency of oscillation. Sample calculations were performed for the delta, convex, and concave wings including a possible space shuttle configuration. The results were compared with those obtained by the slender body theory and by Landahl's theory. The present method obtained more negative damping-in-pitch than that predicted by Landahl's theory. In particular, the present method provides the stability derivatives in the low-frequency range where Landahl's theory breaks down.

Nomenclature

a	= pitch axis location
$A(x)$	= cross-sectional area at station x
$\mathcal{R}$	= aspect ratio = $4\sigma^2/S$
b	= dimensional body length
c	= Euler's constant
$C_{M_q}, C_{M_{\dot{\alpha}}}$	= stability derivatives due to total damping-in-pitch
C_p	= total pressure coefficient
C_{p_o}	= steady-state pressure coefficient
C_{p_1}	= in-phase unsteady pressure coefficient
C_{p_2}	= out-of-phase unsteady pressure coefficient
$f(x, y)$	= oscillation amplitude distribution
$g(x, y)$	= wing thickness distribution
k	= reduced frequency of oscillation
K_1	= modified Bessel function of second kind
L_{ij}	= generalized force coefficient
M	= generalized force coefficient for fundamental solutions
M_∞	= freestream Mach number
r	= $[(y-\eta)^2+z^2]^{1/2}$
$R(x)$	= radius at x of body of revolution
$s(x)$	= $a_1x+a_2x^2$—wing planform shape
S	= wing planform area
t	= nondimensional time
$\bar{t}$	= dimensional time
U_o	= dimensional freestream velocity
w	= $\delta(f_x+ikf)$—downwash
x, y, z	= nondimensional Cartesian coordinates
$\bar{x}, \bar{y}, \bar{z}$	= dimensional Cartesian coordinates
γ	= ratio of specific heats
δ	= oscillation amplitude
ε	= thickness ratio of wing
$\hat{\varepsilon}$	= thickness ratio of body of revolution
σ	= semispan-to-chord ratio
Γ	= parabolic constant
ω	= dimensional frequency
Φ	= transonic small perturbation potential
ϕ	= steady-state potential
φ	= unsteady potential

Presented as Paper 73-122 at the AIAA 11th Aerospace Sciences Meeting, Washington, D.C., January 10–12, 1973; submitted March 13, 1973; revision received October 5, 1973. This study was sponsored by NASA Langley Research Center under Grant NGR-43-001-102 with technical monitoring by J. South, Aerodynamic Loads Division. The authors gratefully acknowledge the assistance of Research Assistant L. Shen in carrying out the computations for this report.

Index categories: Nonsteady Aerodynamics; Subsonic and Transonic Flow.

* Assistant Professor of Mathematics.

† Consultant; presently employed at the University of Southampton, Southampton, England.

‡ Research Associate, also Associate Scientist, Lockheed-Georgia Co., Marietta, Ga.

§ Professor of Aerospace Engineering. Member AIAA.

Introduction

THE small perturbation equation governing transonic flow has become well established. Its use in the prediction of transonic phenomena is greatly complicated by the fact that the equation is nonlinear. The prediction of unsteady phenomena, in particular the stability derivatives, is somewhat less complicated, however, provided the solution to the corresponding steady flow problem is known sufficiently accurately. In this study we show how the recent improvements in the solution of the steady-state case may be used to obtain the thickness effect of the body on its unsteady behavior. Our study is restricted to pointed, low aspect ratio concave, convex, and delta wings oscillating at low frequencies in sonic flow, i.e., $M_\infty = 1$, and at sufficiently low angle of attack to avoid the nonlinear lift effect recently discussed by Cheng and Hafez.[20]

Lin, Reissner, and Tsien[1] showed that the governing equation could be linearized for the two-dimensional case if the reduced frequency of oscillation k is much larger than the $\frac{2}{3}$ power of the thickness ratio ε. Landahl[2,3] linearized the unsteady flow equation assuming high-frequency ($k \gg \varepsilon^2$ for axisymmetric and $k \gg \sigma\varepsilon \ln \sigma^{-1} \varepsilon^{-1/3}$ for three-dimensional) flow oscillation and developed several results for two- and three-dimensional shapes. Hsu and Ashley[4] extended the work of Landahl[2] to blunt-nosed slender bodies performing lateral oscillations. Liu[5] extended Platzer and Hoffman's[6] quasi-slender body theory for supersonic flow using a body-fixed coordinate system for the half body of revolution oscillating at high frequencies in a sonic flow.

More recent work of Teipel[7] and Liu, Platzer, and Ruo[8,9] included the nonlinear term effect in the unsteady potential equation for airfoils[7] and bodies of revolution[8] oscillating in a sonic flowfield by extending Oswatitsch and Keune's[10] parabolic method.

The present study uses a simiar approach to that of Liu for the inclusion of thickness effect via the parabolic constant into the unsteady equation for the case of thin slender wings. Landahl's method is generalized and the Adams-Sears iterative procedure is used to solve the resulting equations.

The parabolic constant Γ is obtained for the wing from the equivalent body of revolution, as required by Oswatitsch's[11]

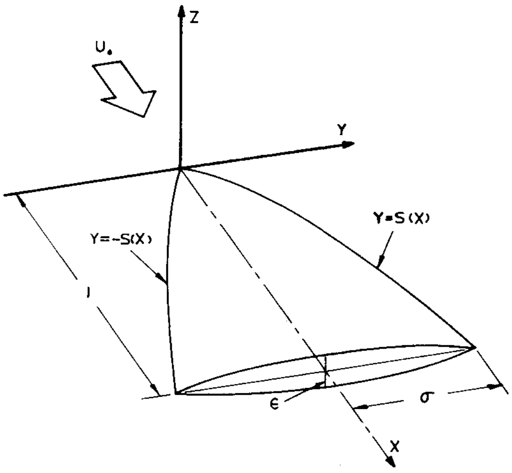

Fig. 1 Coordinate system.

equivalence rule. The parabolic constant for the body of revolution may then be determined by the improved methods of Maeder and Thommen,[12] Alksne and Spreiter,[13] and Hosokawa.[14]

Problem Formulation

Consider a rigid pointed wing which performs harmonic pitching oscillations of small amplitude in a steady uniform transonic flow. It is required that the wing be smooth and sufficiently thin that the conditions for the validity of small perturbation theory are satisfied.

With the flow directed along the positive x axis and the wing oriented along the x axis, we may introduce nondimensional variables x, y, z by the relations $\bar{x} = bx$, $\bar{y} = by$, $\bar{z} = bz$, and $t = (U_o/b)t$, where b is the body length, U_o is the freestream speed, and the bar coordinates are the physical coordinates. The steady-state position of the wing, which for convenience is assumed to be symmetric, is then as shown in Fig. 1. Denoting the thickness ratio by ε, the requirement that the wing be thin becomes $\varepsilon \ll 1$.

Since the shock strength is of order ε^3, we may ignore the rotationality effect of the shock in the solution up to order $\varepsilon^3 \ln \varepsilon$. Consequently, we may assume the existence of a velocity potential Φ such that the x, y, and z components of the flow velocity are $(1+\Phi_x)$, Φ_y, and Φ_z, respectively. It has been shown (e.g., by Landahl[15]) that the potential Φ must satisfy the following equation:

$$(1-M_\infty{}^2)\Phi_{xx}+\Phi_{yy}+\Phi_{zz}-2M_\infty{}^2\Phi_{xt}-M_\infty{}^2\Phi_{tt} = (\gamma+1)M_\infty{}^2\Phi_x\Phi_{xx} \quad (1)$$

Consistent with the requirement that the wing perform small oscillations of amplitude δ about its steady-state position, we may write the equation for points on the wing as

$$z = \varepsilon g(x,y)\,\mathrm{sgn}\,z+\delta\,Re(e^{ikt})f(x,y) \quad (2)$$

where $g(x,y)$ is the steady-state wing shape of order 1 and $f(x,y)$, also of order 1, represents the change in shape due to oscillation. k is the reduced frequency of oscillation equal to $\omega b/U_o$ where ω is the physical frequency. We assume the oscillation to be a small disturbance to the steady-state solution, so $\varepsilon \gg \delta$.

The condition of tangential flow on the body becomes

$$\Phi_z]_{\text{body}} = \varepsilon g_x\,\mathrm{sgn}\,z+\delta(f_x+ikf)\,Re\,e^{ikt}+G(\varepsilon,\delta) \quad (3)$$

where

$$G(\varepsilon,\delta) = \Phi_y]_{\text{body}}(\varepsilon g_y\,\mathrm{sgn}\,z+\delta f_y\,Re\,e^{ikt})$$

Letting σ denote the semispan to chord ratio, we let $\bar{y} = y/\sigma$ in the last term in Eq. (3)

$$G(\varepsilon,\delta) = \Phi_y]_{\text{body}}(\varepsilon\sigma^{-1}g_{\bar{y}}\,\mathrm{sgn}\,z+\delta\sigma^{-1}f_{\bar{y}}\,Re\,e^{ikt}) \quad (4)$$

Then, if the wing is assumed to be nearly planar so that $\sigma \gg \varepsilon$, Eq. (4) is negligible and the boundary condition, Eq. (3), becomes

$$\Phi_z]_{\text{body}} = Re\,\{\varepsilon g_x\,\mathrm{sgn}\,z+\delta(f_x+ikf)\,e^{ikt}\} \quad (5)$$

Moreover, we assume that δ is sufficiently small so that Eq. (5) may be evaluated on $z = \pm 0$ instead of Eq. (2).

The Parabolic Method

The nonlinear term in Eq. (1) is the fundamental difficulty in solving the preceding problem. Following the ideas of Lin, Reissner, and Tsien,[1] Landahl showed that the nonlinear term would be negligible for k sufficiently high, i.e., $k \gg \sigma\varepsilon \ln \sigma^{-1}\varepsilon^{-1/3}$. This restricts the range of validity and leaves out completely the effect of body thickness as the equations for the unsteady part of the potential are then completely independent of the steady-state solution. For the steady-state case for the body of revolution, Oswatitsch and Keune[10] replaced Φ_{xx} by the parabolic constant Γ. In addition, we confine ourselves to flows for which $M_\infty = 1$, thus the governing equation (1) becomes

$$\Phi_{yy}+\Phi_{zz}-2\Phi_{xt}-\Phi_{tt} = \Gamma\Phi_x \quad (6)$$

Let $\Phi = Re(\varphi\, e^{ikt})+\phi$ where the steady-state potential ϕ satisfies

$$\phi_{yy}+\phi_{zz} = \Gamma\phi_x \quad (7a)$$

$$\phi_z(x,\pm 0) = \varepsilon g_x\,\mathrm{sgn}\,z \quad (7b)$$

Then, the unsteady part φ satisfies

$$\varphi_{yy}+\varphi_{zz}-2ik\varphi_x+k^2\varphi = \Gamma\varphi_x \quad (8a)$$

$$\varphi_z(x,\pm 0) = \delta(f_x+ikf) \quad (8b)$$

If the symmetry with respect to z is noted, then we may consider instead the problem

$$\varphi_{yy}+\varphi_{zz}-(\Gamma+2ik)\varphi_x+k^2\varphi = 0 \qquad \text{for} \quad z>0 \quad (9a)$$

$$\varphi_z(x,y,+0) = \delta(f_x+ikf) \qquad \text{for} \quad |y| < S(x) \quad (9b)$$

$$\varphi(x,y,+0) = 0 \qquad \text{for} \quad |y| \geqq \delta(x) \quad (9c)$$

The parabolic constant is obtained from the steady-state solution, Eq. (7), and it thus introduces the effect of thickness into the unsteady solution to Eq. (9).

Determination of the Parabolic Constant from the Equivalent Body of Revolution

Oswatitsch and Keune,[16] Maeder and Thommen,[12] Alksne and Spreiter,[13] and Hosokawa[14] have introduced and improved methods of determining the parabolic constant for slender parabolic bodies of revolution with radius $R(x) = \hat{\varepsilon}x(2-x)$ and for cones with radius $R(x) = \hat{\varepsilon}x$. Ruo and Liu[8] used these methods to obtain the parabolic constant for the steady-state solution.

It has been shown by Zierep[17] that the equivalence rule (Oswatitsch[11]) between wings and bodies also holds for the parabolic method. In particular, if a wing and a body have the same cross-sectional area at corresponding points on the axis, then their parabolic constants are the same. Thus, we may use the parabolic constant obtained in Eq. (8) for a body of revolution of cross-sectional area $A(x)$ for any wing with the same cross-sectional area.

As illustration, consider the planform modeled after a space shuttle shown in Fig. 2. Although this planform is concave, the equivalent body which we use is a cone with radius $R(x) = \hat{\varepsilon}x$. Thus, the flow is accelerating and the use of the parabolic method is legitimate. It is true, however, that the parabolic method for the cone is less satisfactory than for an ogive body.

Any cross-sectional shape may be used for which the cross-sectional area at x is the same as that of the curve, i.e., $A(x) = \pi\hat{\varepsilon}^2x^2$. In this case, it is convenient to consider a cross section which is a semiellipse. (This readily allows application of the equivalence rule to predict angle-of-attack and camber effects in the steady-state solution following the methods of Heaslett and Spreiter[18] and Spreiter and Stahara.[19] For the equivalent

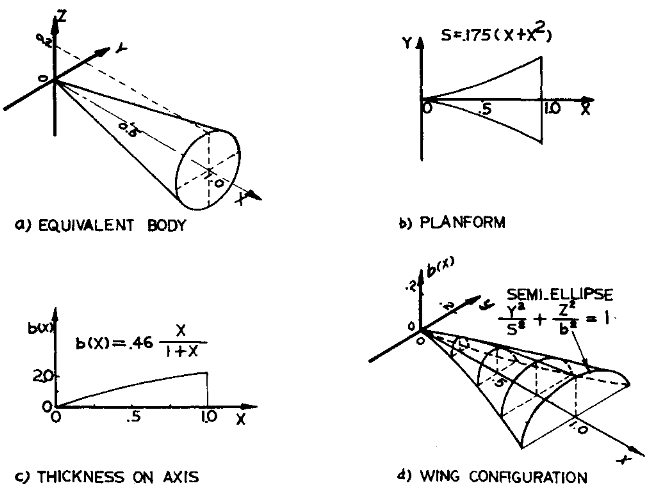

Fig. 2 Space shuttle type body with equivalent cone.

body of revolution, we take the cone with radius $R(x) = \hat{\varepsilon}x$. Then, equating the cross-sectional area of the wing and cone, we obtain

$$A(x) = \tfrac{1}{2}\pi s(x)b(x) = \pi\hat{\varepsilon}^2x^2 \tag{10}$$

where $b(x)$ is the thickness of the wing at the midpoint of the span at the x station and $s(x) = 1/2\sigma x(1+x)$. Therefore, $b(x)$ must have the functional form

$$b(x) = 2\hat{\varepsilon}^2x^2/s(x) = 4\hat{\varepsilon}^2x/\sigma(1+x) \tag{11}$$

Now, since $b(x)$ is monotone increasing and $b(1)$ will be the thickness ratio ε of the wing, $\hat{\varepsilon}$ must be $[b(1)\sigma/2]^{1/2}$ from which the value of Γ may be obtained in curve 1 of Fig. 3.

Note that we have used an unsymmetric wing in this example. No difficulty is encountered here since the unsteady potential equations will be the same for the unsymmetric case as they are for the symmetric case. Obtaining the steady-state solution is more complicated, however. Here the equivalence rule method mentioned previously may be used.

Derivation of the Asymptotic Equations

Equation (9a) can be written

$$\varphi_{yy}+\varphi_{zz}-A\varphi_x+k^2\varphi = 0 \tag{12}$$

where $A = \Gamma+2ik$. Applying the Laplace transform with respect to x gives

$$\hat{\varphi}_{yy}+\hat{\varphi}_{zz}-K^2\hat{\varphi} = 0 \tag{13}$$

where

$$K^2 = A_p-k^2$$

and

$$\hat{\varphi}(p,y,z) = \int_0^\infty \varphi(x,y,z)e^{px}\,dx$$

Green's theorem for the solution of this equation in the upper half plane $z > 0$, p constant, which vanishes at infinity, is

$$\hat{\varphi}(p,y,z) = \frac{1}{\pi}\int_{-\sigma}^{\sigma}\hat{\varphi}(p,\eta,+0)(-K^2)^{1/2}(z/r)K_1[(-K^2)^{1/2}r]\,d\eta \tag{14}$$

where

$$r = [(y-\eta)^2+z^2]^{1/2}$$
$$Re\,p > 0, \qquad Re(-K^2)^{1/2} > 0$$

and K_1 is the Modified Bessel function of the second kind. We can obtain an asymptotic expansion valid for low values of σ by expanding the Bessel function in series for small values of its argument

$$\hat{\varphi}(p,y,z) = \frac{1}{\pi}\int_{-\sigma}^{\sigma}\frac{z\hat{\varphi}}{r^2}d\eta + z\left\{\frac{2}{4\pi}\left(1-2c-2\ln\frac{iK}{2}\right)\cdot \int_{-\sigma}^{\sigma}\hat{\varphi}\,d\eta - \frac{K^2}{2\pi}\int_{-\sigma}^{\sigma}\hat{\varphi}\ln r\,d\eta - \frac{K^4}{32\pi}\left(\frac{5}{2}-2c-2\ln\frac{iK}{2}\right)\cdot \int_{-\sigma}^{\sigma}\hat{\varphi}r^2\,d\eta + \frac{K^4}{16\pi}\int_{-\sigma}^{\sigma}\hat{\varphi}r^2\ln r\,d\eta\right\} + 0[(\sigma k)^6\hat{\varphi}] \tag{15}$$

where c = Euler's constant = 0.5772.

In order to satisfy the boundary condition Eq. (9b) we differentiate Eq. (15) with respect to z and let $z \to 0$ to obtain

$$\hat{\varphi}_z(p,y,+0) = -\frac{1}{\pi}\int_{-\sigma}^{\sigma}\frac{\hat{\varphi}_\eta}{y-\eta}d\eta + \frac{K^2}{4\pi}\left[\left(1-2c-2\ln\frac{i}{2}\right)\cdot \int_{-\sigma}^{\sigma}\hat{\varphi}\,d\eta - 2\int_{-\sigma}^{\sigma}\ln|y-\eta|\,\hat{\varphi}\,d\eta\right] - \frac{K^4}{32\pi}\left[\left(\frac{5}{2}-2c-2\ln\frac{iK}{2}\right)\int_{-\sigma}^{\sigma}(y-\eta)^2\hat{\varphi}\,d\eta - 2\int_{-\sigma}^{\sigma}(y-\eta)^2\ln|y-\eta|\,\hat{\varphi}\,d\eta\right] \tag{16}$$

Inverting Eq. (16) term by term gives

$$w = -\frac{1}{\pi}\oint_{-s}^{s}\frac{\varphi_\eta}{y-\eta}d\eta + P^{(1)}[\varphi] + P^{(2)}[\varphi] \tag{17}$$

where

$$P^{(1)}[\varphi] = \frac{1}{4\pi}(l-1)D\int_{-s}^{s}\varphi(x,\eta)\,d\eta - \frac{1}{4\pi A}D^2\cdot \int_0^x e^{k^2(x-\xi)/A}\ln(x-\xi)\int_{-s}^{s}\varphi(\xi,\eta)\,d\eta\,d\xi + \frac{1}{2\pi}D\int_{-s}^{s}\ln|y-\eta|\,\varphi(x,\eta)\,d\eta \tag{18}$$

$$P^{(2)}[\varphi] = \frac{1}{32\pi}\left(l-\frac{5}{2}\right)D^2\int_{-s}^{s}(y-\eta)^2\varphi(x,\eta)\,d\eta - \frac{1}{32\pi A}D^3\int_0^x e^{k^2(x-\xi)/A}\ln(x-\xi)\int_{-s}^{s}(y-\eta)^2\varphi(\xi,\eta)\,d\xi\,d\eta + \frac{1}{16\pi}D^2\int_{-s}^{s}(y-\eta)^2\ln|y-\eta|\,\varphi(x,\eta)\,d\eta \tag{19}$$

while $D = A\,\partial/\partial x-k^2$, $1 = \ln(A/4)+c$, and $w = \varphi_z(x,y,0+)$.

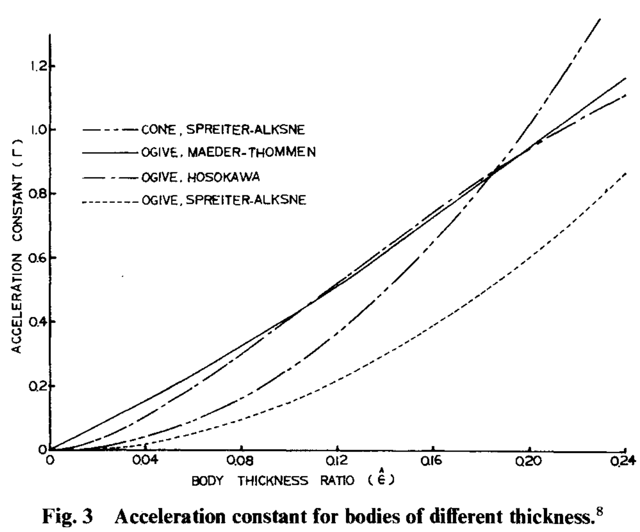

Fig. 3 Acceleration constant for bodies of different thickness.[8]

Adams-Sears Solution of the Asymptotic Equations

The Adams-Sears iteration technique consists in letting

$$\varphi = \varphi^{(0)}+\varphi^{(1)}+\varphi^{(2)}+\cdots$$

where, $\varphi^{(0)}$ is the Jones slender wing solution satisfying

$$w = -\frac{1}{\pi}\oint_{-s}^{s}\frac{\varphi_\eta^{(0)}}{y-\eta}d\eta \tag{20}$$

and $\varphi^{(1)}$, $\varphi^{(2)}$ satisfy

$$0 = -\frac{1}{\pi}\oint_{-s}^{s} \frac{\varphi_\eta^{(1)}}{y-\eta} d\eta + P^{(1)}[\varphi^{(0)}] \tag{21}$$

$$0 = -\frac{1}{\pi}\oint_{-s}^{s} \frac{\varphi_\eta^{(2)}}{y-\eta} d\eta + P^{(1)}[\varphi^{(1)}] + P^{(2)}[\varphi^{(2)}] \tag{22}$$

These Söhngen integral equations are then readily solved, provided the wing is pointed and

$$\varphi^{(n)}[x, s(x)] = \varphi^{(n)}[x, -s(x)] = 0, \qquad n = 0, 1, 2 \tag{23}$$

Let Q be the operator defined by

$$Q[F(x,\mu)] = \int_{-s}^{y} \frac{1}{\pi(s^2-v^2)^{1/2}} \oint_{-s}^{s} \frac{-F(x,\mu)(s^2-\mu^2)^{1/2}}{v-\mu} d\mu\, dv \tag{24}$$

Then

$$\varphi^{(0)} = Q[-w(x,\mu)] \tag{25a}$$

$$\varphi^{(1)} = Q\{P^{(1)}[\varphi^{(0)}(x,\mu)]\} \tag{25b}$$

$$\varphi^{(2)} = Q\{P^{(1)}[\varphi^{(1)}(x,\mu)]\} + Q\{P^{(2)}[\varphi^{(0)}(x,\mu)]\} \tag{25c}$$

We restrict ourselves to wing planforms of form $s(x) = a_1x + a_2x^2$ and to functions w depending only on x. Then, we find

$$\varphi^{(0)} = -\, w(s^2-y^2)^{1/2} \tag{26}$$

$$\begin{aligned}\varphi^{(1)} = &-\tfrac{1}{8}(s^2-y^2)^{1/2}[(l-1)D(ws^2) + (\tfrac{2}{3}y^2+\tfrac{1}{3}s^2)Dw + \\ &2D[ws^2(\ln s/2 - \tfrac{1}{2})] - \textstyle\int_0^x D(ws^2)'\ln(x-\xi)\,d\xi - \\ &k^2ws^2 + 0(k^4)\end{aligned} \tag{27}$$

$$\begin{aligned}Q\{P^{(2)}[\varphi^{(0)}]\} = &-(1/1536)(s^2-y^2)^{1/2}[\![(6l-15)\cdot \\ &[(\tfrac{4}{3}y^2+\tfrac{2}{3}s^2)D^2(ws^2) + D^2(ws^4)] + 8(\tfrac{1}{5}y^4 + \tfrac{1}{10}y^2s^2 + \\ &\tfrac{3}{40}s^4)D^2w + 12(\tfrac{4}{3}y^2+\tfrac{2}{3}s^2)D^2(ws^2) + 3D^2(ws^4) + \\ &12(\tfrac{4}{3}y^2+\tfrac{2}{3}s^2)D^2[ws^2\ln(s/2)] + 12D^2[ws^4\ln(s/2)] - \\ &6(\tfrac{4}{3}y^2+\tfrac{2}{3}s^2)\textstyle\int_0^x D^2(ws^2)'\ln(x-\xi)\,d\xi - \\ &6\textstyle\int_0^x D^2(ws^4)'\ln(x-\xi)\,d\xi - 6A(\tfrac{4}{3}y^2+\tfrac{2}{3}s^2)\ln x[D(ws^2)']_{x=0} - \\ &6k^2(\tfrac{4}{3}y^2+\tfrac{2}{3}s^2)D(ws^2) - 6k^2D(ws^4) + 0(k^4)]\!]\end{aligned} \tag{28}$$

In order to deal with $Q[P^{(1)}(\varphi^{(1)})]$ we split $\varphi^{(1)}$ into two parts

$$\varphi^{(1)} = \alpha(x)(s^2-y^2)^{1/2} + \beta(x)y^2(s^2-y^2)^{1/2} \tag{29}$$

where the definitions of α and β follow from Eq. (27). Then, we obtain

$$\begin{aligned}Q[P^{(1)}(\varphi^{(1)})] = &Q\{P^{(1)}[\alpha(s^2-y^2)^{1/2}]\} + \\ &Q\{P^{(1)}[\beta y^2(s^2-y^2)^{1/2}]\}\end{aligned} \tag{30}$$

where

$$\begin{aligned}Q\{P^{(1)}[\beta y^2(s^2-y^2)^{1/2}]\} = &-(1/384)(s^2-y^2)[\![(l-1)s^3\cdot \\ &(sD^2w + 4As'Dw) + 4D^2w(\tfrac{1}{5}y^4 + \tfrac{1}{10}y^2s^2 + \tfrac{3}{40}s^4) - \\ &4s^2D^2w(\tfrac{1}{3}y^2+\tfrac{1}{6}s^2) + 2s^4[\ln(s/2)+\tfrac{1}{4}]D^2w - \\ &8ss'ADw(\tfrac{1}{3}y^2+\tfrac{1}{6}s^2) + 8As^3s'Dw[\ln(s/2)+\tfrac{1}{2}] - \\ &\textstyle\int_0^x D(s^4Dw)'\ln(x-\xi)\,d\xi - k^2s^4Dw + 0(k^4)]\!]\end{aligned} \tag{31}$$

and

$$\begin{aligned}Q\{P^{(1)}[\alpha(s^2-y^2)^{1/2}]\} = &\tfrac{1}{8}A(s^2-y^2)^{1/2}[\tfrac{2}{3}y^2\alpha' + \\ &m\alpha's^2 + m\alpha(s^2)' - \tfrac{5}{3}\alpha's^2 - \alpha(s^2)' - \\ &\textstyle\int_0^x(\alpha s^2)''\ln(x-\xi)\,d\xi] - \tfrac{1}{8}k^2(s^2-y^2)^{1/2}[\tfrac{2}{3}y^2\alpha + \\ &m\alpha s^2 - \tfrac{2}{3}\alpha s^2 - \textstyle\int_0^x(\alpha s^2)'\ln(x-\xi)\,d\xi]\end{aligned} \tag{32}$$

where $m = 1 + \ln(s^2/4)$.

After attempts were made to substitute α, α', and α'' in formula (32), it was decided that the work would be more accurate if these formulae were computer coded and executed, thereby alleviating the chance of human error. In addition, it was found that the term

$$\textstyle\int_0^x(\alpha s^2)''\ln(x-\xi)\,d\xi \tag{33}$$

includes an integral of form

$$I = \textstyle\int_0^x \xi\ln s(\xi)\ln(x-\xi)\,d\xi \tag{34}$$

which cannot be evaluated in closed form unless s corresponds to the delta wing, i.e., $a_2 = 0$.

The singular behavior of many of the terms in the preceding formulae point up the difficulty of direct numerical evaluation from the start. Now, however, we need numerically integrate only terms affecting the second-order correction. Moreover, we know the form of singularity in the integrand. This allowed us to design a numeric integration routine to correctly compute the singular integrals.

Fundamental Solutions

We consider two types of oscillations which the wing may perform:

Plunging

$$\varphi = \varphi_1;\quad f(x,y) = 1;\quad w = \delta ik \tag{35a}$$

Pitching about an axis $x = a$

$$\varphi = \varphi_2;\quad f(x,y) = x-a;\quad w = \delta[1+(x-a)ik] \tag{35b}$$

Both types of motion can be made up of the superposition of two fundamental solutions to Eq. (9), namely

$$\varphi_A \text{ corresponding to } w(x) = 1 \tag{36a}$$

and

$$\varphi_B \text{ corresponding to } w(x) = x \tag{37}$$

Then

$$\varphi_1 = \delta ik\varphi_A \tag{38}$$

and

$$\begin{aligned}\varphi_2 &= \delta(1-aik)\varphi_A + \delta ik\varphi_B \\ &= \varphi_2 - a\varphi_1\end{aligned} \tag{39}$$

Pressure Coefficient and Generalized Forces

The pressure coefficient may be obtained as for example in Landahl[15] from expansion of Bernoulli's equation. Neglecting squared terms this gives

$$\begin{aligned}C_p &= -2\Phi_x - 2\Phi_t \\ &= -2(\phi_x+\phi_t) - Re[2e^{ikt}(\varphi_x + ik\varphi)] \\ &= C_{p_0} + \delta C_{p_1}\cos kt + \delta C_{p_2}\sin kt\end{aligned} \tag{40}$$

where

$$\begin{aligned}C_{p_1} &= -(2/\delta)(Re\,\varphi_x - k\,Im\,\varphi) \\ C_{p_2} &= -(2/\delta)(-Im\,\varphi_x - k\,Re\,\varphi)\end{aligned} \tag{41}$$

and C_{p_1} and C_{p_2} represent the in-phase and out-of-phase pressure coefficients.

We define the generalized aerodynamic force coefficients by

$$L_{ij} = (4/S\delta_i)\textstyle\int\int_S[\varphi_{i,x} + ik\varphi_i]_{z=0} f_j\,dx\,dy \tag{42}$$

where S is the wing planform area, the displacement distribution function for harmonic oscillations in mode j is given by $f_j(x,y)\cos kt$ (f_j is of order 1), and φ_i is the unsteady potential due to mode i.

It is possible to obtain the L_{ij} for pitching and plunging in terms of those for the fundamental solutions φ_A and φ_B. Since these will be evaluated numerically and φ_x is singular at the wing leading edge, we integrate Eq. (42) by parts to obtain

$$L_{ij} = \frac{8}{S\delta_i}\left[ik\int_0^1\int_0^{s(x)} \varphi_i f_j\,dx\,dy - \int_0^1\int_0^{s(x)} \varphi_i f_j'\,dx\,dy + \int_0^{s(1)} \varphi_i(1,y)\,dy\right] \tag{43}$$

In order to obtain the moments for φ_A and φ_B we require

$$M_{A1} = \int_0^1\int_0^{s(x)} \varphi_A\,dx\,dy \tag{44a}$$

$$M_{Ax} = \int_0^1\int_0^{s(x)} \varphi_A x\,dx\,dy \tag{44b}$$

$$M_A = \int_0^{s(1)} \varphi_A(1,y)\,dy \tag{44c}$$

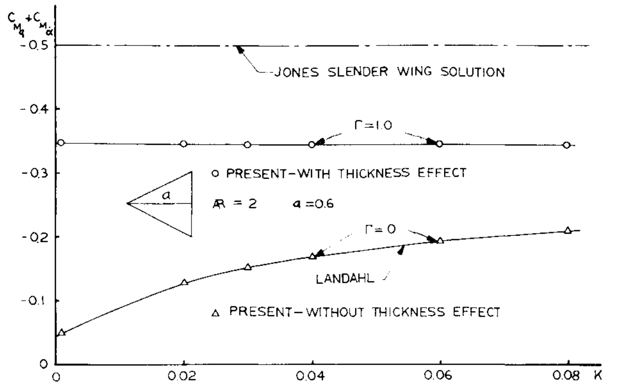

Fig. 4 Comparison of total damping-in-pitch computed by various theories for a delta wing of aspect ratio 2 pitching about $x = 0.6$.

$$M_{B1} = \int_0^1 \int_0^{s(x)} \varphi_B \, dx \, dy \tag{44d}$$

$$M_{Bx} = \int_0^1 \int_0^{s(x)} \varphi_B x \, dx \, dy \tag{44e}$$

$$M_B = \int_0^{s(1)} \varphi_B(1, y) \, dy \tag{44f}$$

Then denoting the plunging mode by $i, j = 1$ and the pitching mode by $i, j = 2$, we have

$$L_{11} = (8/S)ik[ikM_{A1} + M_A] \tag{45a}$$

$$L_{12} = (8/S)ik[ikM_{Ax} - M_{A1} + M_A] \tag{45b}$$

$$L_{21} = (8/S)[ik(M_{A1} + ikM_{B1}) + (M_A + ikM_B)] \tag{45c}$$

$$L_{22} = (8/S)[ik(M_{Ax} + ikM_{Bx}) - (M_{A1} + ikM_{B1}) + (M_A + ikM_B)] \tag{45d}$$

The stability derivatives are defined in terms of the L_{ij} as for example in Landahl. We will be most interested in the total damping-in-pitch for a wing oscillating about axis $x = a$ where $0 \leq a \leq 1$. This is given by (Landahl[15] p. 17)

$$C_{M_q} + C_{M_{\dot{\alpha}}} = (1/k) \, Im[L_{22} - a(L_{21} + L_{12}) + a^2 L_{22}] \tag{46}$$

Basic Wing Configurations

To illustrate the effect of body geometry and thickness effect, i.e., parabolic constant Γ influence, numerical examples were calculated for three basic wing planforms. They are 1) Delta Wing: $s(x) = \sigma x$; 2) Convex Wing: $s(x) = \sigma(2x - x^2)$; and 3) Concave Wing: $s(x) = \frac{1}{2}\sigma(x + x^2)$.

Total damping-in-pitch for pitching oscillations about $x = 0.6$ was computed to illustrate typical behavior of the dynamic stability derivatives and these were compared with results obtained earlier by Landahl without thickness effect.

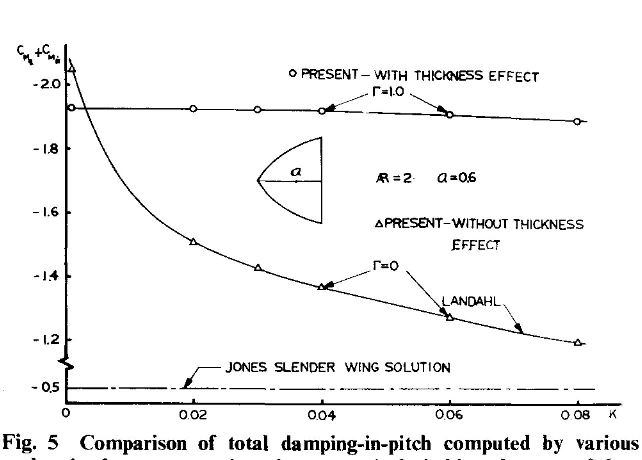

Fig. 5 Comparison of total damping-in-pitch computed by various theories for a convex wing of aspect ratio 2 pitching about $x = 0.6$.

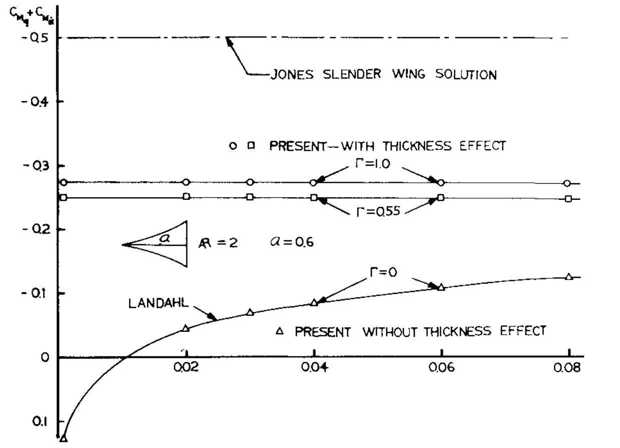

Fig. 6 Influence of thickness effect on damping-in-pitch for delta, convex, and concave wings oscillating about $x = 0.6$ with reduced frequency $k = 0.03$.

Discussion of Results

Total damping-in-pitch was computed and plotted for the various wing planforms vs acceleration constant Γ and reduced frequency k. The Γ values for the concave shuttlelike configuration were chosen from the Spreiter-Alksne curve in Fig. 3 for a wing of semi-span to chord ratio $\sigma = 0.35$ and for a maximum thickness of 0.23 which gives the thickness ratio for the equivalent body of revolution, a cone of radius $\hat{\varepsilon} = 0.2$ and parabolic constant $\Gamma = 1.0$.

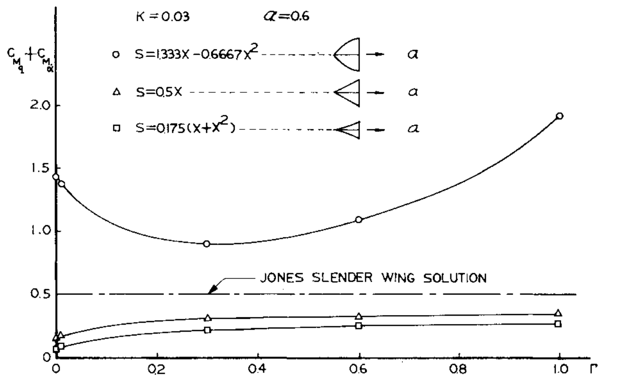

Fig. 7 Comparison of total damping-in-pitch computed by various theories for a concave wing of aspect ratio 1.7 pitching about $x = 0.6$.

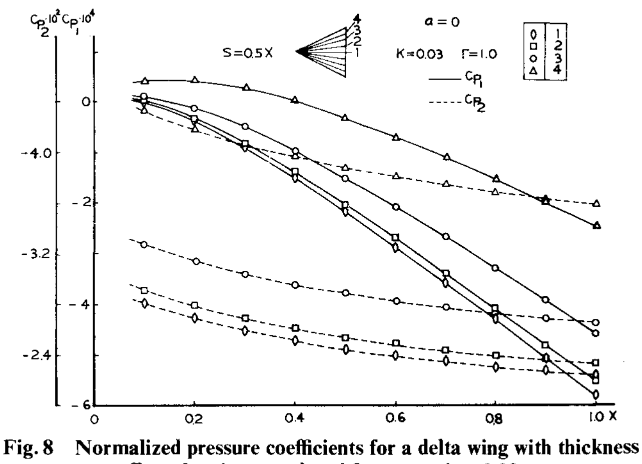

Fig. 8 Normalized pressure coefficients for a delta wing with thickness effect plunging at reduced frequency $k = 0.03$.

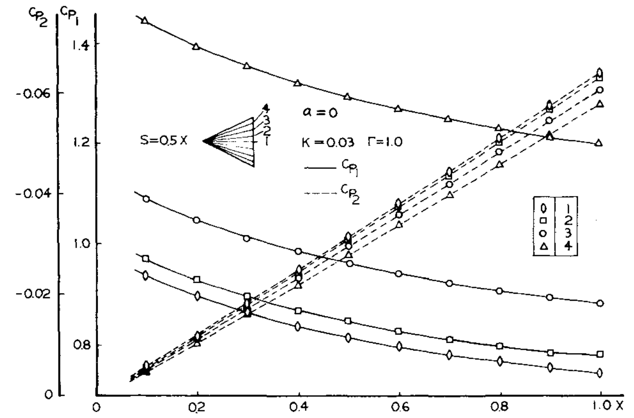

Fig. 9 Normalized pressure coefficients for a delta wing with thickness effect pitching about $x = 0$ at reduced frequency $k = 0.03$.

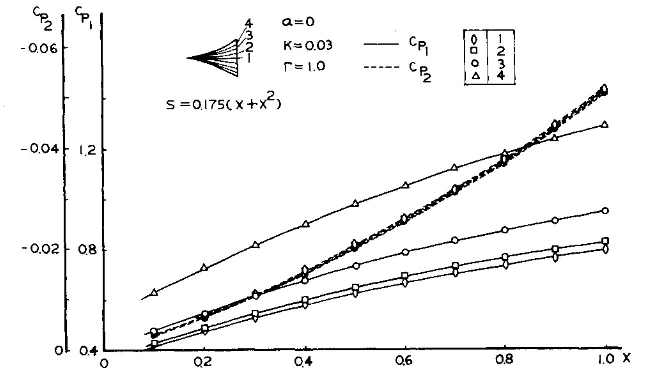

Fig. 12 Normalized pressure coefficient for a concave wing with thickness effect pitching about $x = 0$ at reduced frequency $k = 0.03$.

Calculations of the unsteady potential and stability derivatives have been carried out for various values of Γ between 0 and 1.0. Application of these results may be made to many different wing configurations of a fixed planform. The thickness distribution of the wing is restricted only by the requirement that the cross-sectional area at each x station equals that of the equivalent body of revolution.

Values of Γ may be found from Fig. 3, curve 1 for any wing equivalent to a cone with radius $R(x) = \hat{\varepsilon}x$ and hence cross-sectional area $A(x) = \pi\hat{\varepsilon}^2x^2$. Three theories have been developed for ogive bodies of revolution with $R(x) = \hat{\varepsilon}x(2-x)$ and cross-sectional area $A(x) = \pi\hat{\varepsilon}^2x^2(2-x)^2$. At present Hosokawa's method (Curve 3) seems to give the best values of Γ for the steady-state solution.

For computations in which $\Gamma = 1.0$ the following applications can be made: 1) Any wing for which the cross-sectional area is $A(x) = 0.126x^2$. Equivalent body-of-revolution is a cone of radius 0.02. 2) Using the Maeder-Thommen theory (Curve 2), any wing of cross-sectional area $A(x) = 0.138x^2(2-x)^2$. 3) Using the Hosokawa (Curve 3), any wing of cross-sectional area $A(x) = 0.144\ x^2(2-x)^2$. 4) Using the Alksne-Spreiter theory (Curve 4), any wing of cross-sectional area $A(x) = 0.246x^2(2-x)^2$.

This example shows the additional refinement of the steady-state parabolic method is needed to more closely determine the best choice of parabolic constant.

In Fig. 4, the damping-in-pitch is compared for a delta wing with $\Gamma = 1.0$ to the values predicted by Jones and Landahl. Note that when $\Gamma = 0$, the Landahl case is obtained as it should be. But whereas Landahl shows decreasing damping as frequency gets small, the present method shows little frequency variation in the low range. This may be due to thickness effect. Thus, the decrease in damping predicted by Landahl's method is not predicted by the present parabolic method.

Figure 5 shows that the solution with thickness effect for a convex wing also predicts increasing damping and hence increasing stability as frequency becomes small just as Landahl's method did. However, the amount of damping is generally higher than Landahl's except at the lower frequency limit where Landahl's solution becomes infinite, but the present solution approaches a finite value as expected. This excessively high damping is partially due to a high value of Γ and becomes much

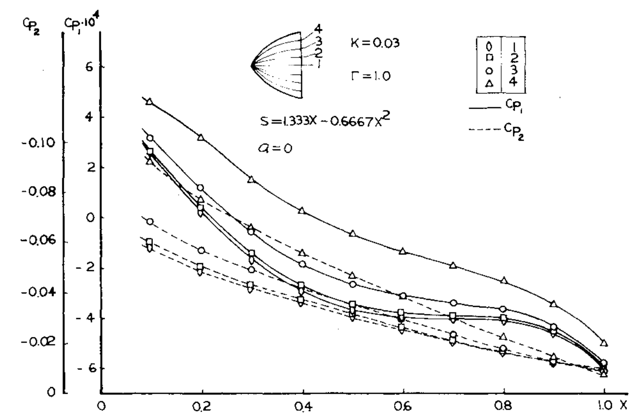

Fig. 10 Normalized pressure coefficient for a convex wing with thickness effect plunging at reduced frequency $k = 0.03$.

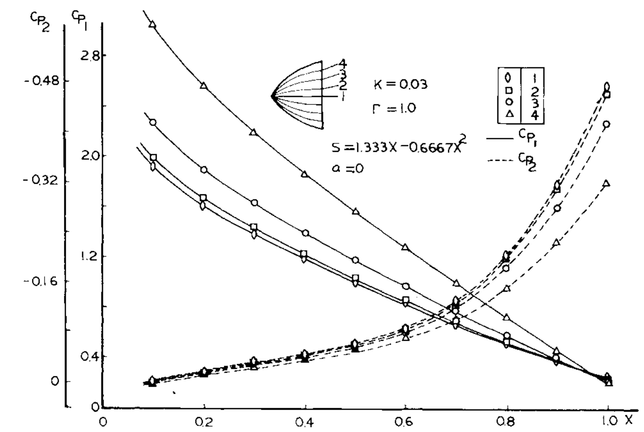

Fig. 11 Normalized pressure coefficient for a convex wing with thickness effect pitching about $x = 0$ at reduced frequency $k = 0.03$.

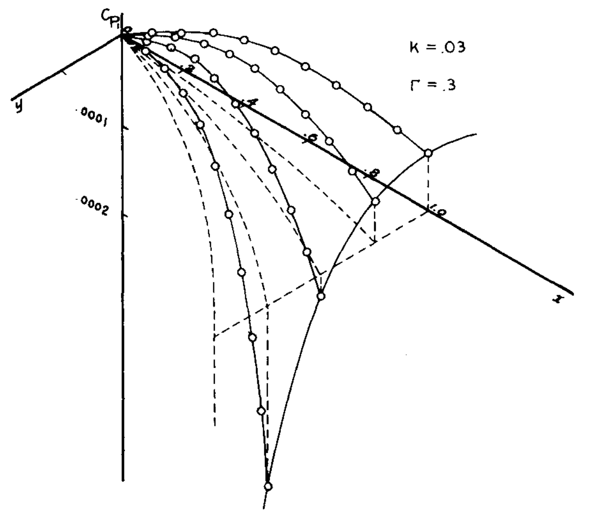

Fig. 13 In-phase normalized pressure coefficient for a concave wing with thickness effect plunging at reduced frequency $k = 0.03$.

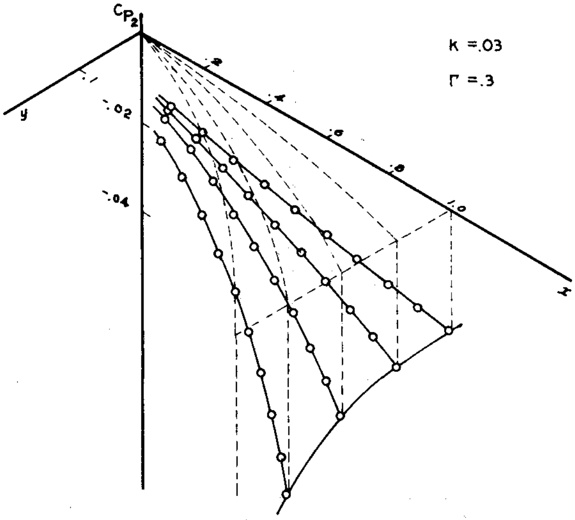

Fig. 14 Out-of-phase normalized pressure coefficient for a concave wing with thickness effect plunging at reduced frequency $k = 0.03$.

less pronounced when Γ is taken near 0.3 instead of 1.0 as can be seen from Fig. 6.

Figure 7 illustrates even more dramatically the difference which thickness effect makes in the low-frequency range. The concave wing, which Landahl's solution implies is unstable for low frequency, as found to be stable by the present method.

Figure 6 shows the effect of different body thicknesses on stability. Note that there is little change in dependence on thickness effect over a wide range for the delta and concave wings. But the convex wing shows quite different behavior. Its stability increases as thickness becomes small and as thickness becomes large with a minimum near $\Gamma = 0.3$. The physical reason for this behavior is not yet fully understood.

Figures 8–12 show the pressure coefficients in-phase C_{p_1} and out-of-phase C_{p_2}, for each of the wing planforms at the frequency $k = 0.03$. Figures 13 and 14 show a three-dimensional plot of in-phase and out-of-phase pressure for the plunging concave wing.

References

[1] Lin, C. C., Reissner, E., and Tsien, H. S., "On Two-Dimensional Non-Steady Motion of a Slender Body in a Compressible Fluid," *Journal of Mathematics and Physics*, Vol. XXVII, 1948, pp. 220–231.

[2] Landahl, M. T., "Forces and Moments on Oscillating Slender Wing-Body Combination at Sonic Speed," OSR TN 56-109, 1956, Office of Scientific Research, Baltimore, Md.

[3] Landahl, M. T., "Linearized Theory for Unsteady Transonic Flow," Rept. 63-2, March 1963, MIT Fluid Dynamics Research Lab., Cambridge, Mass.

[4] Hsu, P. T. and Ashley, H., "Introductory Study of Airloads on Blunt Bodies Performing Lateral Oscillations," Rept. 59-9, 1959, MIT Fluid Dynamics Research Lab., Cambridge, Mass.

[5] Liu, D. D., "Quasi-Slender Body Theory for Unsteady Linearized Transonic Flow Past Pointed Bodies of Revolution," LMSC HREC A791435, April 1968, Lockheed Missiles & Space Co., Huntsville, Ala.

[6] Platzer, M. F. and Hoffman, G. H., "Quasi-Slender Body Theory for Slowly Oscillating Bodies of Revolution in Supersonic Flow," TN D-3440, June 1966, NASA.

[7] Teipel, I., "Die Instationaren Luftkrafte bei der Machzahl 1," *Zeitschrift für Flugwissenschaften*, Bd. 12, Heft 1, 1964, pp. 6–14; also "The Nonsteady Aerodynamic Forces at Mach Number One," translation, RSIC-8-8, 1968, Redstone Arsenal, Ala.

[8] Ruo, S. Y. and Liu, D. D., "Calculation of Stability Derivatives for Slowly Oscillating Bodies of Revolution at Mach 1.0," LMSC HREC D1 62375, Feb. 1971, Lockheed Missiles & Space Co., Huntsville, Ala.

[9] Liu, D. D., Platzer, M. F., and Ruo, S. Y., "On the Calculation of Static and Dynamic Stability Derivatives for Bodies of Revolution at Subsonic and Transonic Speeds," AIAA Paper 70-190, New York, 1970.

[10] Oswatitsch, K. and Keune, F., "Flow Around Bodies of Revolution at Mach Number One," paper presented at Brooklyn Polytechnic Conference on High-Speed Aeronautics, The Polytechnic Institute of Brooklyn, Brooklyn, N.Y., Jan. 20–22, 1955.

[11] Oswatitsch, K., "Similarity and Equivalence in Compressible Flow," *Advances in Applied Mechanics*, Vol. VI, Academic Press, New York, 1955, pp. 248–268.

[12] Maeder, P. F. and Thommen, H. U., "Linearized Transonic Flow About Slender Bodies of Revolution at Zero Incidence," TR WT-25, July 1957, Brown University Div. of Engineering, Providence, R.I.

[13] Spreiter, J. R. and Alksne, A. Y., "Slender Body Theory Based on Approximate Solution of the Transonic Flow Equation," TR-R-2, 1959, NASA.

[14] Hosokawa, I., "A Refinement of the Linearized Transonic Flow Theory," *Journal of the Physical Society of Japan*, Vol. XV, No. 11, 1960, pp. 149–157.

[15] Landahl, M. T., *Unsteady Transonic Flow*, Pergamon Press, New York, 1961.

[16] Oswatitsch, K. and Keune, F., "Ein Äquivalenzsatz für nichtangestellte Flugel kleiner Spannweite in schallnaher Strömung," *Zeitschrift für Flugwissenschaften*, Bd. 3, Heft 2, 1955, Seite 29–46.

[17] Zierep, J., "Der Aquivalenzsatz und die Parabolische Methode für Schallnahe Strömungen," *Zeitschrift für Angewandte Mathematik und Mechanik*, Bd. 45, Heft 1, Seite 19–27.

[18] Heaslet, M. A. and Spreiter, J. R., "Three-Dimensional Transonic Flow Theory Applied to Slender Wings and Bodies," TR 1318, 1957, NASA.

[19] Spreiter, J. R. and Stahara, S. S., "Aerodynamics of Slender Bodies and Wing-Body Combinations," *AIAA Journal*, Vol. 9, No. 9, Sept. 1971, pp. 1784–1791.

[20] Cheng, H. K. and Hafez, M. M., "Equivalence Rule and Transonic Flows Involving Lift," *AIAA Journal*, Vol. 11, No. 8, Aug. 1973, pp. 1210–1212.